

## Sol-Gel formation and kinetic analysis of the in-situ/self-seeding transformation of bayerite $[\text{Al}(\text{OH})_3]$ to $\alpha$ -alumina

Joaquín Aguilar-Santillán, Heberto Balmori-Ramírez\* and Richard C. Bradt

Department of Metallurgical and Materials Engineering, The University of Alabama, Tuscaloosa AL, USA 35487-0202

\*Departamento de Ingeniería Metalúrgica, ESIQIE, Instituto Politécnico Nacional - UPALM, A. P. 75-872, México D.F., 07300 México

The sol-gel formation of Bayerite,  $\text{Al}(\text{OH})_3$ , precipitated from  $\text{AlCl}_3 \cdot 6\text{H}_2\text{O}$  (13.6 g/l) and  $\text{NH}_4\text{OH}$  (4N) at a basic pH 9 was studied. The resulting Bayerite was in the form of prisms  $\sim 3 \mu\text{m}$  in length. The transformation of this Bayerite to  $\alpha$ -alumina was  $[\text{Al}(\text{OH})_3] \rightarrow \gamma\text{-Al}_2\text{O}_3 \rightarrow \delta\text{-Al}_2\text{O}_3 \rightarrow \theta\text{-Al}_2\text{O}_3 \rightarrow \alpha\text{-Al}_2\text{O}_3$ . The slowest of these transitions, the one which controls the transformation by nucleation and growth kinetics, is the  $\theta\text{-Al}_2\text{O}_3$  to  $\alpha\text{-Al}_2\text{O}_3$ . This rate-controlling transformation was studied by two different thermal treatments. One was isothermal and the other had two steps, the first of which created "in situ" nuclei, to enhance the transformation rate. The latter treatment reduced the time for the transformation at  $1100^\circ\text{C}$  from  $>80$  h to only  $\sim 13$  h and reduced the activation energy from  $419.02 \text{ kJ mol}^{-1}$  to  $317.52 \text{ kJ mol}^{-1}$ . It produced a finer crystal size of  $\alpha$ -alumina.

**Key words:** Alumina, Sol-Gel Processing, Activation Energy, Thermal Treatments, and Nucleation.

### Introduction

During the last two decades the incorporation of chemical methods into ceramic powder processing has increased. These methods have been applied to produce fine ceramic particles with high purities and with controlled geometries, or shapes. These powders can produce high density ceramic bodies after sintering. In the specific case of alumina, the chemical sol-gel processing route has been studied by several investigators, utilizing organometallic compounds [1-11]. Those compounds can serve as precursors for many types of aluminum hydroxides and aluminum oxides of extraordinarily high purity levels.

Another approach, one with similar results, but using slightly different processing, is the utilization of organic salts. During decomposition, these salts may leave behind some impurities, and they can affect the final microstructural development of the ceramic. However, one of their advantages is a considerably lower initial raw material cost [1]. The stability field of the particular hydroxide using this technical approach depends strongly on the pH of the precipitation solution. For example Salvador-Morales [2] produced a mixture of Bayerite and Boehmite with a  $\text{pH} < 9$ , but observed that only Bayerite formed at a  $\text{pH} > 9$ .

Aluminum hydroxides transform to  $\alpha$ -alumina by a

sequential dehydroxylation reaction process. The transformation sequence involves a number of metastable, non-equilibrium transition aluminum oxides between  $850^\circ\text{C}$  and  $1025^\circ\text{C}$ . These oxides usually produce a  $\theta$ -alumina. Upon further heating the  $\theta$ -alumina transforms to  $\alpha$ -alumina by a nucleation and growth process. This process controls the reaction rate between  $1050\text{-}1150^\circ\text{C}$  over an extended period of time from  $\sim 20$  to  $36$  h [2, 3]. Table 1 is a summary for many of the common alumina transitions. These depend strongly on the pH, the ionic concentration of the salt, the type and concentration of the alkali present, and the aging time.

To understand and to commercially develop the above reactions to produce alumina, researchers have been interested in the rate-controlling step, the slowest step of the transformation process. This depends on the thermodynamic driving force, the atomic mobility, and the heterogeneity of the sample. Different experimental

**Table 1.** Transition reactions for the formation of  $\alpha$ -alumina [3]

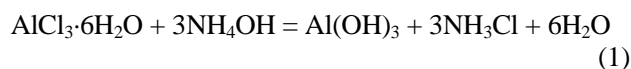
Gibbsite $\rightarrow \chi \rightarrow \kappa \rightarrow \alpha$ .
Gibbsite $\rightarrow$ Boehmite $\rightarrow \gamma \rightarrow \delta \rightarrow \theta \rightarrow \alpha$
Gibbsite $\rightarrow \rho \rightarrow \eta \rightarrow \theta \rightarrow \alpha$
Bayerite $\rightarrow \eta \rightarrow \theta \rightarrow \alpha$
Bayerite $\rightarrow$ Boehmite $\rightarrow \gamma + \delta \rightarrow \theta \rightarrow \alpha$
Bayerite $\rightarrow \rho \rightarrow \eta \rightarrow \theta \rightarrow \alpha$
Boehmite $\rightarrow \gamma \rightarrow \delta \rightarrow \theta \rightarrow \alpha$
Gel $\rightarrow \eta \rightarrow \theta \rightarrow \alpha$
Gel $\rightarrow$ Boehmite $\rightarrow \gamma \rightarrow \delta \rightarrow \theta \rightarrow \alpha$
Diaspore $\rightarrow \alpha$

\*Corresponding author:  
Tel : +1-205-348-0663  
Fax: +1-205-348-2164  
E-mail: Rcbbradt@coe.eng.ua.edu

approaches have been published in the literature. One technique [2] has been to seed fine and high purity  $\alpha$ -alumina particles (of 99.99% of purity and  $0.2 \mu\text{m}$  in size) into a solution of  $AlCl_3 \cdot 6H_2O$  prior to precipitation of the Bayerite gel. This has been suggested to significantly decrease the interfacial surface energy ( $\gamma_{ss}$ ) and the strain energy ( $E_c$ ) required for the nucleation and growth of  $\alpha$ -alumina during the transformation [12, 13]. The temperature and time of transformation are then substantially reduced. Shelleman and Messing [6] have confirmed that the transformation and sintering of a Boehmite gel proceeds much faster when it is seeded with  $\alpha$ -alumina. Another seeding approach has been that by Kao *et al.* [14], who seeded 4% and 17% of  $\alpha$ -alumina ( $0.4 \mu\text{m}$ ) into  $\theta$ -alumina powders ( $\sim 0.058 \mu\text{m}$ ). The amount of seeding improves the transformation to  $\alpha$ -alumina, results that were substantiated by dilatometry.

An alternative process to that of seeding, is one of mechanical activation of the Gibbsite,  $Al(OH)_3$ , by applying the high energy process of attrition milling. During intense attrition milling, the introduction of defects into the particles plays an important role in the rate of the transformation. Jang *et al.* [4] reported that the transformation reaction is completed at a temperature of only  $\sim 875^\circ\text{C}$  and after  $\sim 12$  h at the 99.8% alumina purity level. An apparent disadvantage of this process may be the contamination from the milling media used in the attrition mill.

The present study addresses  $\alpha$ -alumina formation from Bayerite,  $Al(OH)_3$ , which was produced by precipitation from the inorganic salt,  $AlCl_3 \cdot 6H_2O$ . It produces a  $\theta$ -alumina during calcination. The reaction is as follows:



The transformation of the resulting  $\theta$ -alumina to  $\alpha$ -alumina is studied and reported. This study considers the thermal effects during heating to create "in situ" sites for the nucleation of  $\alpha$ -alumina and also the combined effects of size and shape of the Bayerite particles which control the mechanism of the transformation to  $\alpha$ -alumina.

## Experimental Procedures

A Bayerite precipitate was obtained from a mixture of  $AlCl_3 \cdot 6H_2O$  and  $NH_4OH$  solutions with concentrations of 13.6 g/l and 4 N respectively. The process consisted of heating the  $NH_4OH$  solution to  $70^\circ\text{C}$  in the reactor shown in Figure 1, then adding the  $AlCl_3 \cdot 6H_2O$  solution at a constant rate of 6 ml  $\text{minute}^{-1}$ , while a propeller device slowly stirred the system at 10 rpm. The reaction was completed at a pH of 9, a level, which has been reported by Salvador-Morales [2] to be a suitable pH for the stabilization of Bayerite. To

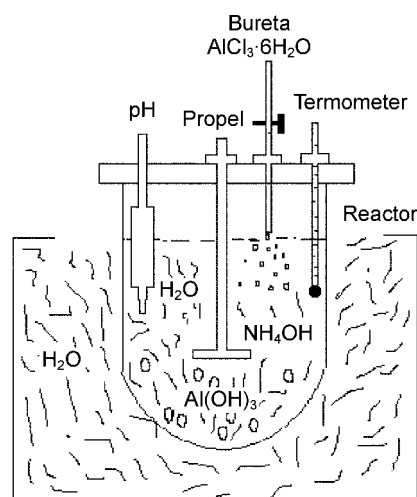


Fig. 1. Reactor to produce the Bayerite,  $Al(OH)_3$ , powders at  $70^\circ\text{C}$ .

homogenize the resulting gel, the system was allowed to age in the "Mother waters" for another 24 h.

Once the gel was aged, it was separated and washed with distilled water using a filter over an Erlenmeyer Flask connected to a vacuum pump. This washing was repeated until all traces of the odor of ammonia disappeared. Carrasco-Mondragon and Balmori-Ramirez [1] reported the total elimination of any  $NH_4Cl$  from the gel once this type of washing eliminated the odor of ammonia. The resulting gel was then dried at  $70^\circ\text{C}$  for 48 h. This dried powder was then manually ground with an agate mortar and pestle until it passed through a -325 mesh sieve. An initial calcination process was applied to this powder by heating at  $10^\circ\text{C minute}^{-1}$  to temperatures of  $750^\circ\text{C}$ ,  $1000^\circ\text{C}$ , and  $1100^\circ\text{C}$  for a holding time of 1 h to calibrate the complete transformation to produce a  $\theta$ -alumina.

To address the transformation kinetics of this  $\theta$ -alumina to  $\alpha$ -alumina, one  $\text{cm}^3$  pellets of the  $\theta$ -alumina were compacted by uniaxial pressing at 128 MPa. The transformation to  $\alpha$ -alumina was then studied for two different thermal treatments:

a) A normal isothermal treatment (ITT) at  $1100^\circ\text{C}$ . Samples were heated at a rate of  $10^\circ\text{C minute}^{-1}$  to  $1100^\circ\text{C}$  then held at this transformation temperature, for different lengths of time. After a partial transformation to  $\alpha$ -alumina, a cooling rate of  $10^\circ\text{C minute}^{-1}$  was applied to room temperature.

b) A two step dynamic thermal treatment (DTT) which included an in-situ "nucleation-like" seeding at  $1150^\circ\text{C}$  was also applied. Samples were first heated at  $10^\circ\text{C minute}^{-1}$ , and then held for 20 minutes at  $1150^\circ\text{C}$  to produce  $\sim 20\%$  of  $\alpha$ -alumina "in-situ" in the  $\theta$ -alumina matrix. A fast cooling rate,  $\sim 100^\circ\text{C minute}^{-1}$ , was then applied to quickly decrease the temperature to  $1100^\circ\text{C}$ . The specimens were then held at  $1100^\circ\text{C}$  for different lengths of time to complete the transformation to  $\alpha$ -alumina, similar to the isothermal heat treatment. After holding at  $1100^\circ\text{C}$ , a cooling rate of  $10^\circ\text{C minute}^{-1}$

was applied to room temperature.

The transformations to  $\alpha$ -alumina in these two thermal treatment processes were monitored by measurements of the specimen densities using Archimedes method, by X-ray diffraction (XRD) using a Siemens D5000 Diffractometer and by Scanning Electron Microscopy using a JEOL 6300 SEM.

## Results and Discussion

The as-formed Bayerite gel lost around 80% of its weight after drying. The diffraction pattern shown in Fig. 2 clearly identifies Bayerite as the hydroxide precipitated at the pH of 9. The morphology and size of the Bayerite powders are shown in Fig. 3, where the fine spherical particles of  $< 1 \mu\text{m}$  diameter with agglomerates of  $\sim 2$  to  $\sim 3 \mu\text{m}$  are the result of the manual grinding. Salvador-Morales [2] reported mixtures of Bayerite and Gibbsite with powder sizes from 1 to 2  $\mu\text{m}$  with irregularities in form. However he added the  $\text{NH}_4\text{OH}$  to the  $\text{AlCl}_3 \cdot 6\text{H}_2\text{O}$  solutions starting from an acid pH, a method that produced the mixture as a result. He also experienced some difficulties to achieve pH's  $> 9$ .

The diffraction patterns of the powders of Bayerite calcined at the three different temperatures are shown in Figure 4. These illustrate a total transformation to  $\theta$ -alumina when the calcining temperature is held at  $1100^\circ\text{C}$  for 1 h. The  $\theta$ -alumina is preceded by two

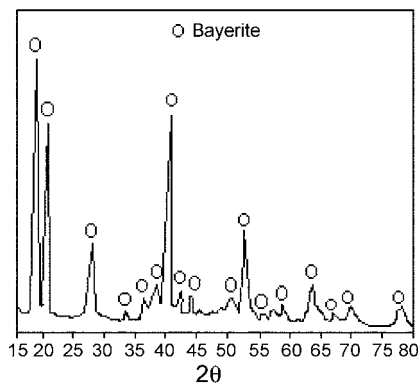


**Fig. 2.** XRD pattern of Bayerite,  $\text{Al}(\text{OH})_3$ , precipitated at a pH of 9.

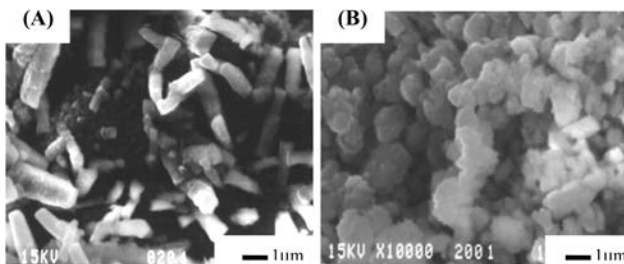


**Fig. 3.** SEM micrographs of the Bayerite,  $\text{Al}(\text{OH})_3$ , powders. The Bayerite obtained by precipitation (A), The Bayerite after manual grinding with an agate mortar and pestle (B).

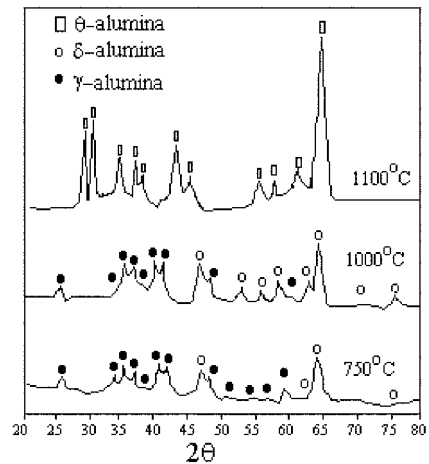


**Fig. 4.** X-ray diffraction patterns following the transformation from Bayerite,  $\text{Al}(\text{OH})_3$  to  $\theta$ -alumina for one hour of heating at  $750^\circ\text{C}$ ,  $1000^\circ\text{C}$  and  $1100^\circ\text{C}$ .

phases:  $\gamma$ -alumina at  $< 750^\circ\text{C}$  and  $\delta$ -alumina at  $< 1000^\circ\text{C}$ . Both of these were formed during the transformation reaction from Bayerite. Similar results have been reported by Salvador-Morales [2] and by Wefers and Misra [3].

The diffraction patterns in Fig. 5(A) illustrate the phase evolution for the isothermal treatment (ITT) which included different transformation times: 1, 2, 6, 9, 27.7, and 83.3 hours. The longest time (83.3 h) was to insure the complete transformation to  $\alpha$ -alumina. Fig. 5(B) illustrates the phase evolution for the dynamic thermal treatment (DTT) which incorporated the short nucleation time at  $1150^\circ\text{C}$  to produce  $\sim 20\%$  of  $\alpha$ -alumina "in-situ" in the  $\theta$ -alumina matrix. This nucleation time of 20 minutes was kept constant during the DTT treatments. Subsequent isothermal transformations at  $1100^\circ\text{C}$  were applied for times of 0.25, 0.5, 3, 9, 11 and 13 hours after the  $1150^\circ\text{C}$  in-situ nucleation seeding step. Again the longest time (13 h) was to insure the

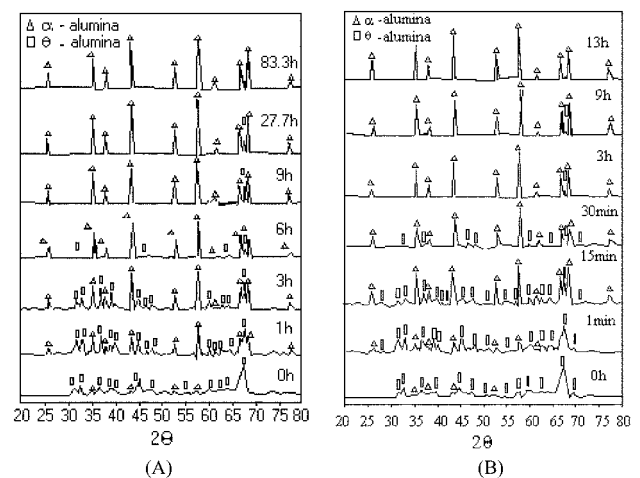


**Fig. 5.** X-ray diffraction patterns following the transformation from  $\theta$ -alumina to  $\alpha$ -alumina for the ITT treatment (A) and the DTT treatment (B) at  $1100^\circ\text{C}$ .

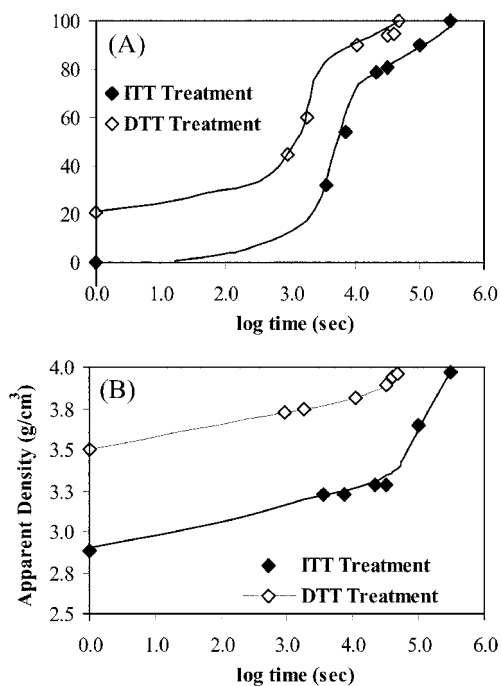


**Fig. 6.** Quantitative analysis obtained by XRD (A). Apparent densities of the two types of samples fired at different firing times at 1100°C (B).

complete transformation to  $\alpha$ -alumina.

The dynamic thermal treatment (DTT) with in-situ seeding creates a much more rapid transformation to  $\alpha$ -alumina than the simple isothermal treatment (ITT). The rate of transformation to  $\alpha$ -alumina is  $\sim 6x$  faster. A quantitative analysis of the  $\alpha$ -alumina phase formation is presented in Fig. 6. Quantitative results are compared with the results of the apparent density of the samples fired at the previous temperature in Fig. 7.

Quantitative analysis substantiates the results from the apparent density. The total transformation density is close to the theoretical value of  $3.98 \text{ g/cm}^3$  for  $\alpha$ -alumina as shown in Fig. 6. This confirms that the transformation is 100% complete. The two thermal processes are different in the variation in their apparent density and global porosity. Figure 7(A) shows the apparent density as a function of the  $\alpha$ -alumina content. Unfortunately, the global densities are not comparable, because of the excessive open porosity in the samples. Besides, the open porosity does not decrease, the global density and the apparent density both increase with the amount of  $\alpha$ -alumina present (Fig. 7(B)). This confirms the theoretical volume reduction of  $\sim 10.2\%$  for the transformation from  $\theta$ -alumina to  $\alpha$ -alumina with the crystal structural change from the monoclinic ( $\theta$ -phase) to the hexagonal ( $\alpha$ -phase).

Figure 6 illustrates the difficulty to fully complete the transformation from  $\theta$ -alumina to  $\alpha$ -alumina by the isothermal treatment (ITT). For example, the specimen at 27.7 h for the ITT treatment still contains several percent of  $\theta$ -alumina, while for the DTT treatment the

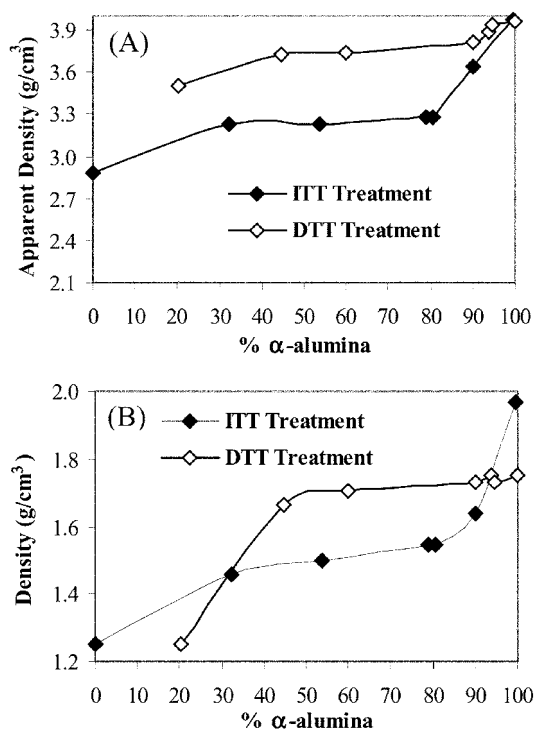


**Fig. 7.** Archimedes densities as a function of the  $\alpha$ -alumina content. Apparent densities (A), and global densities (B).

transformation is 100% complete after only 13 h at 1100°C. The in-situ seeding (DTT) process produces a much higher rate of the transformation that occurs within shorter times than for the isothermal treatment (ITT).

The microstructures of fracture surfaces observed by SEM are illustrated in Fig. 8. From these, the average grain size was estimated to be about  $0.5 \mu\text{m}$  for the DTT treatment and  $1 \mu\text{m}$  for the ITT treatment. Although both structures contain clusters or agglomerates the grain size of the DTT specimens is definitely finer. The DDT thermal treatment not only transforms more readily, it also produces a finer grain size.

## Kinetic Analysis

Although the above analyses present a qualitative estimation of the  $\alpha$ -alumina formation, a kinetic analysis of the process of transformation at different

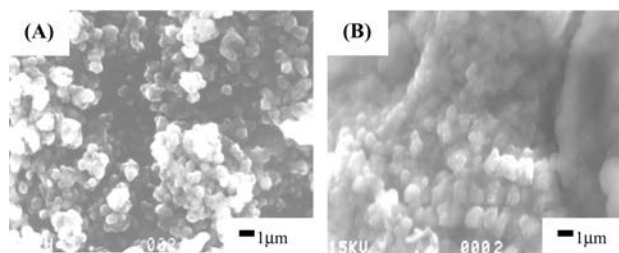


**Fig. 8.** Fracture surfaces of the  $\alpha$ -alumina obtained by the DTT treatment  $\sim 13\text{h}$  (A), and by the ITT treatment  $\sim 83.3\text{h}$  (B) at 1100°C.

temperatures for both the ITT and the DTT thermal treatments is desirable. From Fig. 6(A), it is evident that the transformation rate curves are sigmoidal. These curves suggest typical Avrami-type transformation kinetics [7]. Therefore, the Avrami equation may be used to quantify the transformation for the two different thermal treatments. The volume fraction of the  $\alpha$ -alumina product phase after the time  $t$  is given by:

$$\alpha = 1 - \exp(-K t)^n \quad (2)$$

The exponent,  $n$ , is a constant that depends on the details of the nucleation and growth mechanisms.  $K$  is the rate constant. For isothermal conditions, taking natural logarithms and rearranging yields:

$$\ln[\ln(1/(1-\alpha))] = n \ln K + n \ln t \quad (3)$$

From Equation (3) it is evident that a plot of  $\ln[\ln(1/(1-\alpha))]$  versus  $\ln t$  will enable estimates for the values of both  $n$  and  $K$ . The slope directly produces the  $n$ -value, which can then be incorporated to estimate the  $K$ -value. The plots of Equation 3 for the two thermal treatments are illustrated in Fig. 9. Both treatments yield straight lines. The reaction rate constants for the overall transformation of the Bayerite to  $\alpha$ -alumina follow the Arrhenius relationship:

$$K = A \exp(-Q/RT) \quad (4)$$

where  $A$  is a constant,  $Q$  is the activation energy,  $R$  is the gas constant, and  $T$  is the absolute temperature. A plot of  $(\ln K)$  vs  $(1/T)$  then yields the activation energy for the  $\theta \rightarrow \alpha$  transformation. These results are shown in Fig. 10 and in Table 2.

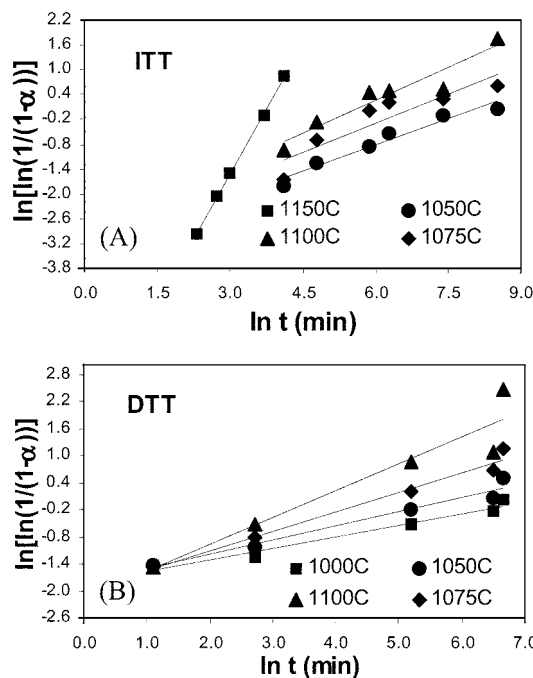


**Fig. 9.** Plot of  $\ln[\ln(1/(1-\alpha))]$  versus  $\ln t$  for formation of  $\alpha$ -alumina by the ITT treatment at 1150°C, 1100°C and 1050°C (A); and the DTT treatment at 1100°C, 1050°C and 1000°C (B).

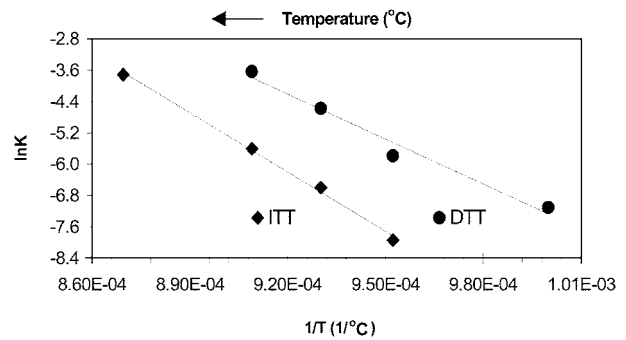


**Fig. 10.** Arrhenius plots for the  $\alpha$ -alumina transformation by the ITT and DTT heat treatments applied in this study.

**Table 2.** Kinetic data from the ITT and DTT heat treatments at different temperatures

ITT	$n$	$K$	$Q$ [kJ mol <sup>-1</sup> ]
1150°C	2.0970	0.0245	419.02
1100°C	0.5885	0.0037	
1075°C	0.4672	0.0014	
1050°C	0.4225	0.0004	
DTT	$n$	$K$	$Q$ [kJ mol <sup>-1</sup> ]
1100°C	0.5955	0.0266	317.52
1075°C	0.4340	0.0103	
1050°C	0.3184	0.0031	
1000°C	0.2568	0.0008	

The isothermal heat treatment (ITT) at 1150°C produces a transformation at the 90% level, after only 60 minutes (Table 2). The mechanism of transformation at 1150°C has a much higher  $n$ -value than the transformations at lower temperatures. This implies a change in the nucleation conditions. However, linearity is still followed when the rate of transformation by the Arrhenius relationship is plotted in Fig. 10. The activation energies suggest that a different mechanism of the  $\theta$ -alumina to the  $\alpha$ -alumina transformation exists for the DTT heat treatment (317.2 kJ mol<sup>-1</sup>) than that needed by the ITT heat treatment (419.02 kJ mol<sup>-1</sup>). The activation energies appear to be reduced as a direct result of the nucleation step, as it is included in the transformation constant,  $K$  (Table 2), which is consistently larger for the DTT heat treatment.

Published activation energies for other studies are summarized in Table 3. This table has the values for both the untreated and the treated powders, either by seeding or milling. Note that, the summary reveals wide ranges of reported activation energies. For the “untreated” transformation, the activation energies range from 419 kJ mol<sup>-1</sup> to 676 kJ mol<sup>-1</sup>. This range appears to be too great for simple experimental variability. There must be a technical explanation. If one refers to the individual studies, then it is evident that not all of the different  $\theta$ -aluminas, which these researchers studied, was prepared in the same way. It is reasonable to conclude that this is the reason for the wide range of

**Table 3.** Activation energies reported for different studies for the  $\theta \rightarrow \alpha$  alumina transformation by nucleation and growth

Researcher	Method	Activation energy, Q (kJ mol <sup>-1</sup> )
Salvador-Morales [2]	3.5% of $\alpha$ -alumina seeding in Bayerite/unseeded	606/661
Jang <i>et al.</i> [4]	Attrition milled gibbsite/unmilled	442/481
Pach <i>et al.</i> [15]	12% of alumina seeding/unseeded***	330/485
Kao and Wei [16]	3/17.5 mol % of alumina seeding	650±1.5/650±50
Yen <i>et al.</i> [17]	0.5 % of alumina seeding/unseeded (Nucleation process)	68.2/171.4
Yen <i>et al.</i> [17]	0.5 % of alumina seeding/unseeded. (Growth process)	580.3/676.2
Shelleman <i>et al.</i> [18]	$\alpha$ -alumina seeding in Boehmite/unseeded***	350/600
McArdle and Messing [19]	$\alpha$ -Fe <sub>2</sub> O <sub>3</sub> seeding in Boehmite/unseeded***	476/600
Bagwell and Messing [20]	$\alpha$ -alumina seeding in Boehmite/unseeded***	350/567
Steiner <i>et al.</i> [26]	Unseeded***	486±21
This study	Thermal in-situ seeding/unseeded	317.52/419.02

\*\*\* $\gamma \rightarrow \alpha$  alumina

activation energies. Essentially the researchers are reporting results for different structural and microstructural  $\theta$ -alumina materials.

A similar wide range of values exists for the treated powders of  $\theta$ -alumina (seeded or milled). It varies from 318 kJ mol<sup>-1</sup> to 650 kJ mol<sup>-1</sup>. However, there is a distinct trend. With the single exception of the Kao and Wei [16] study, all of the references report considerably lower activation energies after the corresponding treatment of the powders, either by seeding or milling procedures. The largest differences from the treated and untreated powders are those by Shelleman *et al.* [18], McArdle and Messing [19] and Bagwell and Messing [20] who started with a  $\gamma$ -alumina. This  $\gamma$ -alumina must have passed through the  $\theta$ -alumina form to create  $\alpha$ -alumina. In any event, it is apparent that creating nuclei, either by seeding or milling procedures, consistently reduces the activation energy of the transformation of  $\theta$ -alumina to  $\alpha$ -alumina.

The transformation from  $\theta \rightarrow \alpha$ -alumina by the DTT heat treatment promotes formation of transformation sites for “in situ” nucleation. This increases the overall rate of the transformation by creating sites of  $\alpha$ -alumina to promote growth. As this reaction is one of nucleation and growth, this suggests that the nucleation step may be the most difficult step in the transformation process [2, 4, 15, 17-20]. The different approaches also suggest that the seeding reduces the interfacial energy as well as the strain energy required to nucleate  $\alpha$ -alumina in the  $\theta$ -alumina matrix [17]. It is clear that the reaction after nucleation is controlled by a growth mechanism, likely by both interfacial and diffusion processes. The rate can be increased, if the temperature is increased, however, coarsening processes will occur which will subsequently affect the final microstructure [18].

The “in situ” seeding of the process by the DTT heat treatment does not appear to directly affect the intrinsic rate of crystal growth. This is because of the time present at 1100°C. In both cases the microstructure is

homogeneous, with a uniform grain size. However, the end grain size is much finer for the DTT treatment, ~0.5  $\mu$ m, versus ~1  $\mu$ m for the isothermal treatment.

## Summary and Conclusions

Nanosized (<1  $\mu$ m) high purity Bayerite,  $Al(OH)_3$ , was produced by the sol-gel method, mixing solutions of  $NH_4OH$  and  $AlCl_3 \cdot 6H_2O$  at a pH=9. The transformation of this Bayerite to  $\alpha$ -alumina was studied for two different thermal treatments, one isothermal (ITT) and the other an “in-situ” seeding (DTT) two-step process. This study reveals that the DTT two-step thermal treatment has a lower activation energy, only 317.52 kJ mol<sup>-1</sup>. That is much less than for the isothermal treatment (ITT), which was 419.02 kJ mol<sup>-1</sup>. However, both results are lower than those studies reported previously by several other researchers (Table 3). This study agrees with other researchers in which they also consistently observed reduced activation energies for seeded or otherwise treated material.

These results suggest that the activation energy for the isothermal transformation may be a mixture of nucleation and growth processes, one that is dependent on the structural details of the  $\theta$ -alumina. The results are in general agreement with previous studies. These have concluded that the transformation occurs by nucleation and growth processes and that the activation energies for isothermal transformation and unseeded or unmilled transformations are consistently larger.

The rate of transformation to  $\alpha$ -alumina also appears to be affected by the initial state or structure, which relates to the number of stable nuclei that are present. It also depends on the type of thermal treatment, as well as the size and shape on the powders produced in the prior precipitation. The in-situ seeding DTT heat treatment described in this work presents an alternative thermal treatment to direct seeding, one that enhances the rate of complete transformation to  $\alpha$ -alumina and produces a very fine crystal size of  $\alpha$ -alumina.

## Acknowledgments

This work was partially supported by the Instituto Politecnico Nacional through the project "Processing Ceramic Oxides DEPI-920398" at the Department of Metallurgical Engineering ESIQIE, Mexico City, 07300 Mexico. Portions of the study were completed while Heberto Balmori-Ramírez was on sabbatical leave at The University of Alabama.

## References

1. L. Carrasco-Mondragon and H. Balmori-Ramírez, Proceedings of the XV Annual Meeting of Metallurgy Research, pp. 1-20 (In Spanish.), Saltillo Coah, Mexico, (1993).
2. A. Salvador-Morales, "Study of the Transformation Kinetics of a Bayerite Gel to  $\alpha$ -alumina with and without Seeds". (In Spanish), M Sc. Thesis with Specialization in Metallurgical Engineering, pp. 14-45, ESIQIE-IPN, Mexico City, Mexico (1996).
3. K. Wefers and C. Misra, Alcoa Tech Report # 9, Alcoa Tech Center, PA, USA (1987).
4. Serk-Won Jang, Heon Young Lee, Kun-Chul Shin, and Sung-Mal Lee, *J. Ceram. Proc. Res.* 2[2] (2001) 67-71.
5. P.D. Exter, L. Winnubst, Theo Yand A. J. Burggr, *J. Am. Ceram. Soc.* 77[9] (1994) 2376-80.
6. R.A. Shelleman and G.L. Messing, *J. Am. Ceram. Soc.* 71[5] (1988) 317-322.
7. W.D. Kingery, H.K. Bowen, and D.R. Uhlmann, "Introduction to Ceramics", pp. 320-447, Wiley Interscience-Second edition, New York, NY, USA (2000).
8. C.J. Brinker and G.W. Sherer, "Sol-Gel Science: The Physics and Chemistry of Sol-Gel Processing", pp. 589-609, Academic Press, New York, NY, USA (1990).
9. D.W. Richerson, "Modern Ceramic Engineering", pp. 125-256, Marcel Dekker Inc., New York, NY, USA (1982).
10. V. Sarasmati, G.V.N. Rao, and G.V.R. Rao, *J. Mater. Sci.* 22 (1987) 529-534.
11. J. Aguilar-Santillán, "Influence of the Heat Treatment in the Kinetics and Grain Size of  $\alpha$ -alumina Transformed from  $\theta$ -alumina Obtained by Calcination of Bayerite", (In Spanish.), B Sc. Thesis in Metallurgical Engineering, pp. 1-32, ESIQIE-IPN, Mexico City, Mexico (1997).
12. H. Balmori-Ramírez and A. Salvador M, *Key Eng. Mats.* 69 (1997) 132-136.
13. D.A. Porter and K.E. Easterling, "Phase Transformation in Metals and Alloys", pp. 263-283, Van Nostrand Reinhold (Int.) Co., Berkshire, England (1981).
14. H.C. Kao, W.J. Wei, and C.Y. Huang, *J. Ceram. Proc. Res.* 4[1] (2003) 34-41.
15. L. Patch, R. Roy, and W.C. Wei, *J. Mater. Res.* 5[2] (1990) 278-285.
16. H.C. Kao and W.C. Wei, *J. Am. Ceram. Soc.* 83[2] (2000) 362-368.
17. F.S. Yen, H.S. Lo, H.L. Wen, and R.J. Yang, *J. Cryst. Growth* 249 (2003) 283-293.
18. R.A. Shelleman, G.L. Messing, and M. Kumagai, *J. Non-Cryst. Sols.* 82[1-3] (1986) 277-285.
19. J.L. McArdle and G.L. Messing, *J. Am. Ceram. Soc.* 76[1] (1993) 214-222.
20. R.B. Bagwell and G.L. Messing, *J. Am. Ceram. Soc.* 82[4] (1999) 825-832.
21. S.J. Wilson and J.D.C. McConnell, *J. Solid State Chem.* 34[3] (1980) 315-322.
22. H.L. Wen and F.S. Yen, *J. Crystal Growth* 208 (2000) 696-708.
23. I.M. Tjburg, H. Debruin, H.P.A. Elberse, and W. Geus, *J. Mater. Sci.* 26 (1991) 5945-5950.
24. M. Kumagai and G.L. Messing, *J. Am. Ceram. Soc.* 68 (1985) 500-505.
25. M. Kumagai and G.L. Messing, *J. Am. Ceram. Soc.* 67 (1984) C230-C231.
26. C.J.P. Steiner, D.P.H. Hasselman, and R.M. Spriggs, *J. Am. Ceram. Soc.* 54[8] (1971) 412-413.